Research Square

Preprints are preliminary reports that have not undergone peer review.
They should not be considered conclusive, used to inform clinical practice,
or referenced by the media as validated information.

Evaluation of Implant Placement Accuracy and CBCT–Surface Comparison Residuals in a Static Implant Surgical-Guide Workflow Using Dental Models

Jung-Tae Lee
Seoul National University Dental Hospital
Sung-Ho Lee
Seoul National University Dental Hospital
Dayeon Park
Seoul National University Dental Hospital
Ye-Seul Jung
Seoul National University Dental Hospital
Dohyung Lim
Sejong University
Bongju Kim
bjkim016@gmail.com

Seoul National University Dental Hospital

Article

Keywords: Static computer-aided implant surgery, Implant placement accuracy, Surgical guides, Cone-beam computed tomography, Surface registration, In vitro study

Posted Date: November 18th, 2026

DOI: https://doi.org/10.21203/rs.3.rs-11453901/v1

License: This work is licensed under a Creative Commons Attribution 4.0 International License.
Read Full License

Additional Declarations: No competing interests reported.

Abstract

This *in vitro* study evaluated implant-placement accuracy and cone-beam computed tomography (CBCT)–surface comparison residuals in a static surgical-guide workflow. Seven dental models provided 28 model–region cases for surface comparison; 42 implant positions in five models were evaluated after guided placement. Two observers measured depth and angular deviations three times per position. For each position, the six absolute depth readings and six angular-deviation readings (two observers × three repeats) were averaged separately. Mean absolute axial depth error was 0.369 ± 0.211 mm, and mean angular deviation was 1.864 ± 0.972° (mean ± standard deviation). Forty-one positions (97.6%) met both study-specific placement reference criteria of ≤ 1.0 mm and ≤ 3.5°. Between-observer ICC(A,1) was 0.821 (95% CI, 0.690–0.900) for absolute depth error and 0.794 (95% CI, 0.646–0.884) for angular deviation; Observer 2 showed a repeat-order effect for angular measurements. The mean case-level standard deviation of surface residuals was 0.235 mm. No statistically significant correlations were detected between surface-comparison metrics and placement outcomes across the five matched models (exact two-sided permutation $P \geq 0.083$). These measurements characterize the workflow under controlled model conditions. The small matched sample limits conclusions about the association between surface residuals and placement accuracy.

Introduction

Static computer-aided implant surgery is intended to transfer a digitally planned implant position to the operative field through a surgical guide. Accuracy is commonly described using deviations at the implant entry point and apex, angular deviation, and, in some studies, depth deviation. Systematic reviews and meta-analyses report measurable deviations despite guided placement, while also documenting substantial variation in study design, guide support, clinical setting, and measurement definitions [1–10]. A pooled analysis of static computer-aided implant surgery reported mean deviations of 1.2 mm at the entry point, 1.4 mm at the apical point, and 3.5° in angulation [1]. These estimates provide clinical context but are not universal acceptance limits and are not directly interchangeable with an axial platform-depth measurement. Accuracy estimates from clinical, cadaveric, and *in vitro* studies also differ, which limits direct generalization across settings [6, 8, 10].

CT-to-surface registration links radiographic data with the dental surface representation used during virtual planning. Registration quality can be affected by segmentation, operator decisions, image artefacts, and the choice of registration method; deviations introduced at this stage may be transferred to later steps in the workflow [11–13]. A surface-comparison residual therefore represents the combined output of image conversion, surface acquisition, coordinate transformation, and alignment settings. It should not automatically be interpreted as the isolated error of a registration algorithm or as a substitute for final implant-position deviation [11, 12].

Final placement deviation may also reflect guide seating and stabilization, support configuration, sleeve geometry and clearance, drilling distance, fabrication method, and resin properties [14–20]. Because

errors can accumulate across image acquisition, registration, guide design and manufacture, drilling, and implant insertion, an overall placement assessment characterizes the evaluated workflow as a whole. It cannot identify the contribution of an individual stage unless that stage is measured separately.

Accurate transfer of an implant plan is relevant to the intended prosthetic envelope and the planned relationship to adjacent teeth and anatomical structures [21]. However, clinical benefit should not be inferred from placement accuracy alone. A meta-analysis of randomized trials found lower positional deviations with static computer-aided approaches for some comparisons, while short-term implant survival and patient-reported discomfort were broadly comparable; the evidence for these clinical outcomes was rated as low quality [9]. Individual randomized trials have also shown that clinical performance depends on the support strategy and surgical protocol [22, 23]. Similarly, a retrospective study of implant proximity to the inferior alveolar canal did not establish a universal distance threshold that guarantees the absence of neurosensory complications [24]. Accordingly, accuracy should be reported as a technical outcome and interpreted within the anatomical, prosthetic, and clinical context, rather than as a direct guarantee of safety or treatment success [7, 21].

This study aimed to characterize implant-placement deviations and CT–surface comparison residuals in a static implant surgical-guide workflow evaluated using dental models. The primary outcomes were axial absolute depth error and angular deviation at 42 implant positions. Measurement reproducibility was assessed using repeated measurements by two observers. As a secondary outcome, CT–surface residuals were described across 28 model–region cases from seven dental models. An exploratory model-level analysis examined the association between registration metrics and implant-placement outcomes in the five models represented in both datasets. The study was designed to characterize the evaluated workflow under controlled bench-top conditions; it was not designed to establish clinical safety, clinical effectiveness, or superiority over other implant-placement methods.

Materials and Methods

Study design and dental models

This *in vitro* bench-top study evaluated a static implant surgical-guide workflow using dental models. Seven Hanil Implant Training B dental models (HL-60042; Hanil, Republic of Korea) were used for the CT–surface comparison. Four regions were evaluated per model: two mandibular regions (MD_A and MD_B) and two maxillary regions (MX_A and MX_B), yielding 28 model–region cases.

Implant-placement measurements were obtained from models 01–05 only and comprised 42 implant positions. Models 06 and 07 were used for drilling-accuracy testing and contributed no implant-placement observations to this analysis. The surgical guides were tooth-supported, and no anchor pins were used. Tooth positions were recorded using the FDI two-digit notation. Only non-living dental models were used; no human participants or living animals were involved. Accordingly, this study characterizes

the tested workflow under controlled model conditions and does not estimate clinical performance [8]. An overview of the study workflow is shown in Fig. 1.

CBCT acquisition and optical surface scanning

Pre-placement CBCT acquisition. Before virtual implant planning, all seven dental models (models 01–07) were scanned in their entirety using a Green X 21 CBCT unit (Vatech, Republic of Korea). These pre-placement CBCT datasets were used for CBCT–surface comparison across all seven models (four regions per model; 28 model–region cases) and as the imaging basis for virtual implant planning in models 01–05.

Post-placement CBCT acquisition. After guided implant placement, models 01–05, which comprised the implant-placement accuracy dataset (42 implant positions), were scanned again in their entirety using a Green X 21 CBCT unit (Vatech, Republic of Korea). These post-placement datasets were used to identify and measure the actual implant positions for the placement-accuracy analysis.

The pre- and post-placement scans were acquired using identical settings: 94 kVp, 5.60 mA, an isotropic voxel size of 0.120 × 0.120 × 0.120 mm, and a field of view of 80 × 80 mm. All images were stored in DICOM format.

Before virtual implant planning and guided placement, each of the seven dental models was scanned using a T710 laboratory scanner (Medit, Republic of Korea; manufacturer-reported accuracy, < 4 μm; point spacing, 0.040 mm). For scanning, each dentiform was placed in the dedicated arch tray. The tray geometry constrained the model's position on the scanner's motorized rotating stage, and the scan path was controlled automatically by the scanner software.

Virtual planning, guide fabrication, and implant placement

Virtual implant planning and surgical-guide design were performed using Clever One v1.5.1 (Ewoosoft, Republic of Korea). The guides were fabricated by an external dental laboratory using an ELEGOO Saturn 4 Ultra 16K printer based on masked stereolithography (MSLA), with a nominal XY resolution of 14 × 19 μm, and SG PRINT resin (DSM-SG-O; DSM Holdings, Republic of Korea). The printer's default layer thickness was 50 μm; however, the layer thickness used for this outsourced batch could not be confirmed. Build orientation, washing and post-curing conditions, and post-print dimensional inspection records were unavailable. The guides were not sterilized because they were used only in a non-clinical dentiform experiment and were not intended for patient use.

NeoBiotech implants with a length of 10 mm and diameters of 3.5, 4.0, or 4.5 mm were used (IS33510AP, IS34010AP, and IS34510AP, respectively). The specified guide-sleeve height was 3.50 mm, and the inner diameter was 5.21 mm (SGS70RW-H3.50D5.21; NeoBiotech, Republic of Korea). The guides were tooth-supported and were used without anchor pins. The sleeve-to-drill clearance, sleeve-to-

bone distance, and drilling distance could not be determined from the experimental records available for this study [16–20].

Guide-based drilling and implant placement were performed on dentiform models using the NeoNavi Surgical Guide Kit (NeoBiotech, Seoul, Republic of Korea). The tooth-supported guide was seated on the dentiform, and proper seating was confirmed before drilling; no anchor pins were used. Drilling was performed using the SM3 surgical engine (NAKANISHI, Japan) set to 1,200 rpm and 50 N·cm; implant insertion was performed using the same engine set to 50 rpm and 40 N·cm. The site-specific drilling sequences were as follows: at FDI tooth positions 11 and 32, tissue punching, point drilling, a 3.0 × 7.3-mm drill (T17080114), a 3.0 × 8.5-mm drill (T17080112), and a 3.0 × 10-mm drill (T17080110) were performed sequentially, followed by placement of an IS33510AP implant (3.5 × 10 mm). At positions 14, 25, and 45, tissue punching, point drilling, a 3.5 × 7.3-mm drill (T17080104), a 3.5 × 8.5-mm drill (T17080102), and a 3.5 × 10-mm drill (T17080100) were performed sequentially, followed by placement of an IS34010AP implant (4.0 × 10 mm). At positions 26, 27, 36, 46, and 47, tissue punching, point drilling, a 4.0 × 7.3-mm drill (T17080094), a 3.5 × 8.5-mm drill (T17080092), and a 3.5 × 10-mm drill (T17080090) were performed sequentially, followed by placement of an IS34510AP implant (4.5 × 10 mm). The final insertion torque was adjusted to 30 N·cm using a hand torque wrench. No external irrigation was used during drilling. All procedures were performed by a single dentist (J.-T.L.).

Implant positions in models 01–05 were planned using Clever One v1.5.1 (Ewoosoft, Republic of Korea) based on the pre-placement CBCT datasets. After guided placement, the post-placement CBCT datasets from these five models, comprising 42 implant positions, were analyzed using Ez3D-i 5.5.12 (Ewoosoft, Republic of Korea) to identify and measure the actual implant positions. The planned implant positions and post-placement CBCT data were registered using surrounding anatomical structures that were unchanged by the procedure. Registration was checked in the axial, sagittal, and coronal views by assessing the overlap of the reference structures, and fine adjustment was performed when necessary to achieve final alignment. The same reference criteria and registration procedure were applied to all models. The superior surface of the implant fixture was used as the implant-level reference. For angular measurement, the planned and placed implant axes were aligned parallel in the coronal view, and the absolute angular difference was measured in the sagittal section showing the greatest divergence. Axial depth deviation was measured along the planned implant long axis at the same location used to determine the maximum angular deviation. Two observers independently measured each implant position three times. For each measurement round, cases were displayed without model identifiers in an order generated using a random-number function; a new random order was generated for each round. The observers were blinded to model identity and their previous measurements. Implant position, rather than each individual reading, was the unit of analysis.

Outcome definitions and repeated measurements

Angular deviation was defined as the absolute sagittal-plane angle between the planned and placed implant axes, measured in the sagittal section showing the greatest divergence after the axes had been

aligned parallel in the coronal view. Signed axial depth error was defined as the actual platform position minus the planned platform position, measured along the planned implant axis at the superior surface of the implant fixture and in the section used to determine the maximum angular deviation. Positive values indicated placement deeper than planned, and negative values indicated placement shallower than planned. Each position had six readings (two observers × three repeats). The position-level signed depth error was the arithmetic mean of the six signed readings, and the position-level absolute axial depth error was the arithmetic mean of the six absolute signed readings, mean($|d_i|$). Position-level angular deviation was the arithmetic mean of the six angular readings.

Two study-specific placement reference criteria were used for descriptive classification: an absolute axial depth error of ≤ 1.0 mm and a sagittal-plane angular deviation of ≤ 3.5°. The 3.5° criterion was selected to correspond to the pooled mean angular deviation reported for static computer-assisted implant surgery [1]. The 1.0-mm criterion was used as a study-specific descriptive cutoff; neither criterion was considered a validated clinical acceptance threshold.

CBCT–surface registration and surface-deviation analysis

Within Clever One v1.5.1, the pre-placement CBCT volume was designated as the reference coordinate system for CBCT-to-STL conversion and CT–surface registration. For surface extraction, the operator used the software-displayed voxel-intensity threshold labelled “HU”; voxels at or above the selected value were included. The threshold slider was manually adjusted while visually checking reproduction of the tooth and gingival contours; the displayed values were approximately − 200 to − 100. Because the selected value was not recorded for each case, exact case-specific values are unavailable and minor variation may have occurred. The same operator manually registered the optical surface scan to the pre-placement CBCT-derived surface using an initial three-point alignment followed by fine adjustment.

Surface deviations were quantified using the 3D Compare function in Geomagic Qualify 12 (3D Systems, USA). The optical model scan was designated as the nominal surface, and the CBCT-derived STL was designated as the comparison surface. The direction of deviation was checked against the software display so that the reported sign convention was consistent with the CBCT reference. For each of the 28 model–region cases, the proportion of reported points within ± 0.250 mm was calculated separately. The overall proportion was the unweighted arithmetic mean of the 28 case-specific proportions; each case therefore contributed equally (1/28), regardless of its point count. The nominal tolerance was set to ± 0.250 mm and the critical tolerance to ± 1.000 mm. These were comparison settings, not clinical acceptance thresholds. Because the available reports were limited to the ± 1.000-mm threshold, they do not establish whether any points exceeded this limit or provide the number or maximum magnitude of such points.

Statistical analysis

Continuous outcomes were summarized using means and standard deviations; medians, ranges, 95% confidence intervals, and empirical 95th percentiles were reported where applicable. Tooth-group results were summarized descriptively. Because the 42 implant positions were clustered within five dental models, no inferential comparisons between tooth groups were performed.

Within-observer reproducibility was assessed using two-way random-effects, absolute-agreement intraclass correlation coefficients (ICCs): ICC(A,1) for a single repeat and ICC(A,3) for the mean of three repeats. Between-observer reproducibility was assessed using ICC(A,1), with each observer's mean across three repeats treated as one rating. Two-sided 95% confidence intervals were calculated using the F-based ANOVA procedure for the corresponding absolute-agreement ICCs; the limits for ICC(A,3) were transformed to the three-measure average scale. ICC selection and reporting followed [25, 26]. Repeat-order effects were evaluated separately for each observer using the Friedman test. Statistical analyses were performed using SigmaPlot 14 (Systat Software Inc., San Jose, CA, USA). The model-level values used in the exploratory correlation analyses are provided in Supplementary Table S4.

CBCT–surface outcomes were summarized across the 28 model–region cases. For the exploratory registration–placement analysis, the four regional metrics were averaged within each model, and implant-placement outcomes were averaged across implant positions within that model. Each of the five models represented in both datasets was one analytical unit (n = 5). Associations were assessed using Spearman's rank correlation with exact two-sided permutation tests. These correlations were exploratory and were not used for causal or predictive inference.

During preparation of this manuscript, ChatGPT (OpenAI) was used to assist with English-language drafting and data summarization. The authors reviewed the AI-assisted outputs, verified the reported data and calculations, and take responsibility for the final content.

Results

Study dataset

The implant-placement dataset comprised 42 positions from models 01–05 (8 anterior, 15 premolar, and 19 molar positions). The CT–surface comparison dataset comprised 28 model–region cases from seven models, with four regions evaluated per model. Five models were represented in both datasets and formed the matched set for the exploratory registration–placement analysis.

Overall implant-placement accuracy

Across the 42 implant positions, the mean absolute axial depth error was 0.369 ± 0.211 mm, and the mean angular deviation was 1.864 ± 0.972°. The empirical 95th percentiles were 0.748 mm for absolute depth error and 3.381° for angular deviation. All 42 positions were within the 1.0-mm depth reference, while 41/42 positions (97.6%) were within the 3.5° angular reference. Both references were met

simultaneously at 41/42 positions (97.6%). The sole position exceeding the angular reference was 03_MX FDI 27, with a mean angular deviation of 5.033°; this position was retained in the analysis (Table 1; Supplementary Table S1; Figure 2).

The mean signed depth error across positions was +0.019 ± 0.428 mm (95% CI, −0.114 to +0.153 mm). Twenty-two positions (52.4%) had a positive mean signed error, 19 (45.2%) had a negative mean signed error, and one (2.4%) had a mean error of zero. No position-level mean signed error reached or exceeded ±1.0 mm.

Placement accuracy by tooth group

Mean absolute depth error was 0.452 ± 0.162 mm in the anterior group, 0.287 ± 0.194 mm in the premolar group, and 0.400 ± 0.228 mm in the molar group. Mean angular deviation was 1.633 ± 0.884° for anterior positions, 1.738 ± 0.924° for premolar positions, and 2.061 ± 1.052° for molar positions. All anterior and premolar positions met both study-specific placement reference criteria, as did 18 of 19 molar positions (94.7%) (Table 1).

Measurement reproducibility

For absolute depth error, intraobserver ICC(A,1) was 0.849 (95% CI, 0.764–0.909) for Observer 1 and 0.756 (0.631–0.851) for Observer 2; the corresponding ICC(A,3) values were 0.944 (0.907–0.968) and 0.903 (0.837–0.945). For angular deviation, intraobserver ICC(A,1) was 0.655 (0.503–0.781) for Observer 1 and 0.563 (0.314–0.741) for Observer 2; the corresponding ICC(A,3) values were 0.851 (0.752–0.915) and 0.795 (0.579–0.895). Between-observer ICC(A,1) was 0.821 (0.690–0.900) for absolute depth error and 0.794 (0.646–0.884) for angular deviation (Table 2; Supplementary Table S2).

CT–surface comparison residuals

Across the 28 model–region cases, the mean case-level standard deviation of surface deviation was 0.235 mm. The overall proportion of reported points within ±0.250 mm was 82.2%, calculated as the arithmetic mean of the 28 case-specific proportions, with equal weight assigned to each case. The threshold-limited reports contained 4,015,727 points in total, with 105,953–198,126 points per case (mean, 143,419). Because the analysis was configured with a critical threshold of ±1.000 mm, the available data cannot determine whether any points exceeded ±1.000 mm or quantify the number or maximum magnitude of exceedances.

By region, the mean case-level standard deviation ranged from 0.222 mm in MX_A to 0.252 mm in MD_B. The mean proportion of reported points within ±0.250 mm ranged from 80.0% in MD_B to 83.8% in MX_A. Across all cases, the unweighted means of the case-level positive and negative deviation summaries were +0.181 mm and −0.150 mm, respectively. Regional mean positive deviations ranged

from +0.153 mm in MX_A to +0.201 mm in MD_B, whereas regional mean negative deviations ranged from −0.158 mm in MX_A to −0.136 mm in MD_A (Table 3; Supplementary Table S3; Figure 3).

Exploratory association between registration metrics and placement accuracy

In the five matched models, the mean registration standard deviation was positively correlated with absolute depth error (Spearman's ρ = 0.667; exact two-sided permutation P = 0.267) and angular deviation (ρ = 0.667; P = 0.267). The proportion of reported surface points within ±0.25 mm was negatively correlated with absolute depth error (ρ = −0.600; P = 0.350) and angular deviation (ρ = −0.900; P = 0.083). These model-level estimates are exploratory and, given the small number of models, do not establish either the presence or absence of an association (Table 4; Figure 4; Supplementary Table S4).

Discussion

In this dental-model bench-top evaluation, the mean absolute axial depth error was 0.369 ± 0.211 mm and the mean angular deviation was 1.864 ± 0.972° across 42 implant positions. Forty-one of the 42 positions met both study-specific placement reference criteria. Across the 28 model–region cases, the mean case-level standard deviation of surface deviation was 0.235 mm. The unweighted arithmetic mean of the 28 case-specific proportions within ± 0.25 mm was 82.2%. Because the Geomagic output was limited to a ± 1.0-mm threshold, the available data do not establish whether any surface points exceeded this range. These findings characterize the workflow under the tested model, imaging, software, and manufacturing conditions.

The reported clinical averages for static computer-aided implant surgery—1.2 mm at the entry point, 1.4 mm at the apex, and 3.5° in angulation—provide context for interpreting the present angular result, but they are not directly comparable with the present depth outcome [1]. The present depth measure was an axial displacement of the platform reference point, whereas the literature values at the entry and apical points generally describe three-dimensional positional deviations. Differences in study design, guide support, anatomy, operators, and measurement protocols further limit direct numerical comparison. Clinical and cadaveric studies may also yield different accuracy estimates from controlled *in vitro* studies [6, 8, 10, 13].

The tooth-group summaries showed numerically greater angular deviation in the molar group, and the only position exceeding the study-specific angular criterion was 03_MX FDI 27 (5.033°). These findings are descriptive. Because multiple implant positions were nested within only five models and no model-clustered subgroup analysis was performed, the results do not establish a general tooth-position effect.

The CBCT–surface residuals characterize the combined output of the comparison workflow and do not isolate the error of the registration algorithm. They may reflect CBCT-to-STL conversion, threshold selection, optical surface acquisition, three-point manual alignment and fine adjustment, and the

Geomagic comparison settings. One operator performed the registration; interoperator variability was not assessed. The threshold values are reported as software-displayed CBCT voxel-intensity settings labelled as “HU” and should not be interpreted as calibrated conventional CT Hounsfield units without an appropriate calibration or conversion procedure [27]. Because the comparison output was limited to ± 1.0 mm, deviations beyond this range could not be assessed.

In the exploratory analysis of five matched models, no statistically significant association was identified between the registration metrics and implant-placement errors. The Spearman correlation between registration standard deviation and depth error was 0.667 (exact two-sided permutation P = 0.267); the correlation with angular error was also 0.667 (P = 0.267). The proportion of surface within ± 0.25 mm was negatively correlated with depth error (ρ = −0.600, P = 0.350) and angular error (ρ = −0.900, P = 0.083). Given that only five models were included, these nonsignificant tests do not rule out a potentially meaningful association. Regional registration metrics were aggregated at the model level and could not be matched to individual implant positions; therefore, the analysis is hypothesis-generating and does not establish causation or predictive performance.

Several technical factors may contribute to final placement deviation, including guide seating and stabilization, support configuration, mechanical tolerance, drilling distance, sleeve geometry, manufacturing method, and resin properties [14–20]. *In vitro* studies have reported effects of drilling distance below the sleeve, guide-support length, resin properties, printing method, and sterilization on guide or implant-position accuracy [17–19]. The present study did not independently manipulate or measure each of these factors. It therefore cannot attribute the overall placement deviations—or the higher angular error at 03_MX FDI 27—to any single design or manufacturing feature.

Accurate transfer of an implant plan is clinically relevant because implant position is related to the planned prosthetic envelope and the proximity of anatomical structures [21]. Nevertheless, clinical acceptance should be determined from the individual anatomical and prosthetic context. The study-specific placement reference criteria used here (≤ 1.0 mm for absolute axial depth error and ≤ 3.5° for sagittal-plane angular deviation) are descriptive and should not be interpreted as universal clinical limits. A retrospective study examining a 2-mm distance from the inferior alveolar canal did not find a statistically significant difference in neurosensory outcomes between the distance groups; paresthesia was reported in three cases with zero distance [24]. This finding does not validate a universal 2-mm safety rule; it illustrates why a distance threshold should not be treated as a guarantee. Evidence from randomized trials and their meta-analysis also indicates that improved placement accuracy does not, by itself, establish improved survival or patient-reported outcomes [7, 9, 21–23].

ICC point estimates were numerically higher for depth than for angular measurements in both within-observer and between-observer comparisons (Table 2). A repeat-order effect was detected for Observer 2’s angular measurements (Kendall’s W = 0.282), indicating variation across repeated readings in this dataset. The cause of this variation cannot be determined from the present data and should not be attributed specifically to learning, fatigue, or implant-placement error. The available data also do not

establish that measurement variability caused the relatively large angular deviation at 03_MX FDI 27. The confidence intervals were relatively broad, particularly for the single-measure angular ICCs, so the point estimates should be interpreted with caution.

This study has several limitations. First, it used dental models under controlled conditions and included no patients, biological tissues, or clinical outcomes. Second, the depth outcome was an axial platform displacement and did not capture three-dimensional entry-point or apical displacement, directional lateral deviation, or distance from critical anatomical structures. Third, the CT–surface residual incorporated multiple acquisition and processing steps. Fourth, the registration–placement association was evaluated at the model level in only five matched models. Fifth, Observer 2 showed a repeat-order effect for angular measurement. The ICC confidence intervals treated implant positions as targets and did not account for the clustering of positions within the five dentiform models.

Future studies should include a larger number of models and record each stage of the workflow separately, including image acquisition, segmentation and registration, guide fabrication, guide seating, and final implant coordinates. Where feasible, dimensional inspection of the guide and direct measurement of planned and placed implant positions could help distinguish contributions from individual stages. Separate clinical studies with patient-centered outcomes would be required to assess clinical effectiveness or safety. The present findings are limited to characterizing the tested workflow and to an exploratory assessment of whether CT–surface metrics were associated with implant-placement outcomes.

Conclusion

Within the limitations of this dentiform bench-top study, the tested static surgical-guide workflow produced mean absolute axial depth and angular deviations of 0.369 mm and 1.864° across 42 implant positions. CT-to-surface comparison yielded a mean case-level residual standard deviation of 0.235 mm across 28 model-region cases. The exploratory analysis in five matched models did not establish a statistically significant association between registration metrics and placement outcomes. These findings characterize the tested workflow and do not establish clinical safety, effectiveness, or superiority.

Declarations

Data availability

All data supporting the findings of this study are provided in the article and Supplementary Tables S1–S4.

Funding

This work was supported by the R&D Infrastructure for Technological Innovation (Project Number: RS-2025-12732968) funded by the Ministry of Trade, Industry & Energy (MOTIE, Korea) and Korea Institute for Advancement of Technology (KIAT).

Competing interests

The authors declare no competing interests.

Author contributions

Conceptualization, B.K. and J.-T.L.; methodology, S.-H.L., D.P., D.L., and Y.-S.J.; software, D.P. and Y.-S.J.; validation, J.-T.L.; formal analysis, J.-T.L.; investigation, J.-T.L., D.P. and Y.-S.J.; resources, B.K.; data curation, J.-T.L., S.-H.L., D.P., D.L., and Y.-S.J.; writing—original draft preparation, B.K. and J.-T.L.; writing—review and editing, B.K. and J.-T.L.; supervision, B.K.; funding acquisition, B.K. All authors reviewed and approved the final manuscript.

References

1. Tahmaseb, A., Wu, V., Wismeijer, D., Coucke, W. & Evans, C. The accuracy of static computer-aided implant surgery: a systematic review and meta-analysis. *Clin. Oral Implants Res.* **29** (Suppl. 16), 416–435. https://doi.org/10.1111/clr.13346 (2018).
2. Shi, Y. et al. A systematic review of the accuracy of digital surgical guides for dental implantation. *Int. J. Implant Dent.* **9**, 38. https://doi.org/10.1186/s40729-023-00507-w (2023).
3. Márquez Bautista, N. et al. Accuracy of different systems of guided implant surgery and methods for quantification: a systematic review. *Appl. Sci.* **14**, 11479. https://doi.org/10.3390/app142411479 (2024).
4. Khaohoen, A. et al. Accuracy of implant placement with computer-aided static, dynamic, and robot-assisted surgery: a systematic review and meta-analysis of clinical trials. *BMC Oral Health*. **24**, 359. https://doi.org/10.1186/s12903-024-04033-y (2024).
5. Vartan, N. et al. Accuracy of three-dimensional computer-aided implant surgical guides: a prospective in vivo study of the impact of template design. *Dent. J.* **13**, 150. https://doi.org/10.3390/dj13040150 (2025).
6. Schneider, D., Marquardt, P., Zwahlen, M. & Jung, R. E. A systematic review on the accuracy and the clinical outcome of computer-guided template-based implant dentistry. *Clin. Oral Implants Res.* **20** (Suppl. 4), 73–86. https://doi.org/10.1111/j.1600-0501.2009.01788.x (2009).
7. D'Haese, J., Van de Velde, T., Komiyama, A., Hultin, M. & De Bruyn, H. Accuracy and complications using computer-designed stereolithographic surgical guides for oral rehabilitation by means of dental implants: a review of the literature. *Clin. Implant Dent. Relat. Res.* **14**, 321–335. https://doi.org/10.1111/j.1708-8208.2010.00275.x (2012).

8. Bover-Ramos, F., Viña-Almunia, J., Cervera-Ballester, J., Peñarrocha-Diago, M. & García-Mira, B. Accuracy of implant placement with computer-guided surgery: a systematic review and meta-analysis comparing cadaver, clinical, and *in vitro* studies. *Int. J. Oral Maxillofac. Implants*. **33**, 101–115. https://doi.org/10.11607/jomi.5556 (2018).
9. Tattan, M., Chambrone, L., González-Martín, O. & Avila-Ortiz, G. Static computer-aided, partially guided, and free-handed implant placement: a systematic review and meta-analysis of randomized controlled trials. *Clin. Oral Implants Res.* **31**, 889–916. https://doi.org/10.1111/clr.13635 (2020).
10. Zhou, W., Liu, Z., Song, L., Kuo, C. L. & Shafer, D. M. The accuracy of implant placement with computer-guided surgery in partially edentulous patients and possible influencing factors: a systematic review and meta-analysis. *J. Prosthodont. Res.* **66**, 29–39. https://doi.org/10.2186/jpr.JPR_D_20_00184 (2022).
11. Flügge, T. et al. Registration of cone beam computed tomography data and intraoral surface scans—a prerequisite for guided implant surgery with CAD/CAM drilling guides. *Clin. Oral Implants Res.* **28**, 1113–1118. https://doi.org/10.1111/clr.12925 (2017).
12. Han, Y. T. et al. Comparison of dental surface image registration and fiducial marker registration: an in vivo accuracy study of static computer-assisted implant surgery. *J. Clin. Med.* **10**, 4183. https://doi.org/10.3390/jcm10184183 (2021).
13. Derksen, W., Wismeijer, D., Flügge, T., Hassan, B. & Tahmaseb, A. The accuracy of computer-guided implant surgery with tooth-supported, digitally designed drill guides based on CBCT scans and intraoral scanning: a prospective cohort study. *Clin. Oral Implants Res.* **30**, 1005–1015. https://doi.org/10.1111/clr.13514 (2019).
14. Cassetta, M., Di Mambro, A., Giansanti, M., Stefanelli, L. V. & Barbato, E. How does an error in positioning the template affect the accuracy of implants inserted using a single fixed mucosa-supported stereolithographic surgical guide? *Int. J. Oral Maxillofac. Surg.* **43**, 85–92. https://doi.org/10.1016/j.ijom.2013.06.012 (2014).
15. Cassetta, M., Giansanti, M., Di Mambro, A. & Barbato, E. Accuracy of two stereolithographic surgical templates: a retrospective study. *Clin. Implant Dent. Relat. Res.* **15**, 448–459. https://doi.org/10.1111/j.1708-8208.2011.00369.x (2013).
16. Cassetta, M., Di Mambro, A., Giansanti, M., Stefanelli, L. V. & Barbato, E. Is it possible to improve the accuracy of implants inserted with a stereolithographic surgical guide by reducing the tolerance between mechanical components? *Int. J. Oral Maxillofac. Surg.* **42**, 887–890. https://doi.org/10.1016/j.ijom.2013.01.011 (2013).
17. El Kholy, K., Janner, S. F. M., Schimmel, M. & Buser, D. The influence of guided sleeve height, drilling distance, and drilling key length on the accuracy of static computer-assisted implant surgery. *Clin. Implant Dent. Relat. Res.* **21**, 101–107. https://doi.org/10.1111/cid.12705 (2019).
18. Kessler, A., Le, V. & Folwaczny, M. Influence of the tooth position, guided sleeve height, supporting length, manufacturing methods, and resin E-modulus on the *in vitro* accuracy of surgical implant

guides in a free-end situation. *Clin. Oral Implants Res.* **32**, 1097–1104. https://doi.org/10.1111/clr.13804 (2021).

19. Kessler, A., Dosch, M., Reymus, M. & Folwaczny, M. Influence of 3D-printing method, resin material, and sterilization on the accuracy of virtually designed surgical implant guides. *J. Prosthet. Dent.* **128**, 196–204. https://doi.org/10.1016/j.prosdent.2020.08.038 (2022).
20. Guentsch, A., An, H. & Dentino, A. R. Precision and trueness of computer-assisted implant placement using static surgical guides with open and closed sleeves: an *in vitro* analysis. *Clin. Oral Implants Res.* **33**, 441–450. https://doi.org/10.1111/clr.13904 (2022).
21. Nulty, A. A literature review on prosthetically designed guided implant placement and the factors influencing dental implant success. *Br. Dent. J.* **236**, 169–180. https://doi.org/10.1038/s41415-024-7050-3 (2024).
22. Younes, F. et al. A randomized controlled study on the accuracy of free-handed, pilot-drill guided and fully guided implant surgery in partially edentulous patients. *J. Clin. Periodontol*. **45**, 721–732. https://doi.org/10.1111/jcpe.12897 (2018).
23. Vercruyssen, M. et al. A randomized clinical trial comparing guided implant surgery (bone- or mucosa-supported) with mental navigation or the use of a surgical template in fully edentulous jaws. *J. Clin. Periodontol*. **41**, 717–723. https://doi.org/10.1111/jcpe.12231 (2014).
24. Tufekcioglu, S., Delilbasi, C., Gurler, G., Dilaver, E. & Ozer, N. Is 2 mm a safe distance from the inferior alveolar canal to avoid neurosensory complications in implant surgery? *Niger J. Clin. Pract.* **20**, 274–277. https://doi.org/10.4103/1119-3077.183240 (2017).
25. Koo, T. K. & Li, M. Y. A guideline of selecting and reporting intraclass correlation coefficients for reliability research. *J. Chiropr. Med.* **15**, 155–163. https://doi.org/10.1016/j.jcm.2016.02.012 (2016).
26. McGraw, K. O. & Wong, S. P. Forming inferences about some intraclass correlation coefficients. *Psychol. Methods*. **1**, 30–46. https://doi.org/10.1037/1082-989X.1.1.30 (1996).
27. Mah, P., Reeves, T. E. & McDavid, W. D. Deriving Hounsfield units using grey levels in cone beam computed tomography. *Dentomaxillofac Radiol.* **39**, 323–335. https://doi.org/10.1259/dmfr/19603304 (2010).

Tables

Table 1. Implant-placement accuracy overall and by tooth group.

Tooth group	n	Absolute axial depth error (mm), mean ± SD	Angular deviation (°), mean ± SD	Both study-specific placement reference criteria met, n/N (%)
Anterior	8	0.452 ± 0.162	1.633 ± 0.884	8/8 (100.0)
Premolar	15	0.287 ± 0.194	1.738 ± 0.924	15/15 (100.0)
Molar	19	0.400 ± 0.228	2.061 ± 1.052	18/19 (94.7)
Overall	42	0.369 ± 0.211	1.864 ± 0.972	41/42 (97.6)

Values are means ± standard deviations across implant positions. Absolute axial depth error is the mean of the six absolute signed readings for each position; angular deviation is the mean of six readings (two observers × three repeats). The study-specific placement reference criteria were ≤1.0 mm for absolute axial depth error and ≤3.5° for angular deviation; these are not universal clinical acceptance thresholds.

Table 2. Within-observer and between-observer measurement reliability.

Outcome	Observer 1 ICC(A,1) (95% CI)	Observer 1 ICC(A,3) (95% CI)	Observer 2 ICC(A,1) (95% CI)	Observer 2 ICC(A,3) (95% CI)	Between-observer ICC(A,1) (95% CI)
Absolute axial depth error	0.849 (0.764–0.909)	0.944 (0.907–0.968)	0.756 (0.631–0.851)	0.903 (0.837–0.945)	0.821 (0.690–0.900)
Angular deviation	0.655 (0.503–0.781)	0.851 (0.752–0.915)	0.563 (0.314–0.741)	0.795 (0.579–0.895)	0.794 (0.646–0.884)

Values are reported as ICC estimates (95% confidence intervals). Within-observer ICC(A,1) and ICC(A,3) were calculated from the three repeat measurements for each observer. Between-observer ICC(A,1) was calculated using each observer's mean across the three repeats. All ICCs used a two-way random-effects model with absolute agreement and were based on 42 implant positions.

Table 3. CBCT–surface comparison residuals by region.

Region	n cases	Mean positive deviation (mm)	Mean negative deviation (mm)	Mean case-level SD (mm)	Surface within ±0.25 mm (%)
MD_A	7	+0.177	-0.136	0.225	82.5
MD_B	7	+0.201	-0.154	0.252	80.0
MX_A	7	+0.153	-0.158	0.222	83.8
MX_B	7	+0.191	-0.153	0.239	82.4
Overall	28	+0.181	-0.150	0.235	82.2

Values are unweighted arithmetic means of the case-level summaries (seven cases per region; 28 cases overall). The percentage within ±0.250 mm is the unweighted mean of the case-specific percentages, with each case given equal weight. The 28 reports represented 4,015,727 points in total (105,953–198,126 per case; mean, 143,419). The comparison was threshold-limited at ±1.000 mm; counts and maximum magnitudes beyond this threshold could not be determined. The tolerances are comparison settings, not clinical acceptance thresholds. Positive deviation denotes the optical surface outside the CBCT-derived STL; negative deviation denotes it inside. MD, mandible; MX, maxilla; A, bilaterally tooth-bounded region; B, posterior free-end region.

Table 4. Exploratory model-level associations between registration metrics and placement outcomes.

Registration metric	Placement outcome	Spearman ρ	Exact two-sided permutation P	n models
Mean CT–surface SD	Absolute axial depth error	+0.667	0.267	5
Mean CT–surface SD	Angular deviation	+0.667	0.267	5
Surface within ±0.25 mm (%)	Absolute axial depth error	−0.600	0.350	5
Surface within ±0.25 mm (%)	Angular deviation	−0.900	0.083	5

Each model was one analytical unit. Registration metrics were averaged across four model–region cases; placement outcomes were averaged across implant positions within the same model. The analysis was exploratory (five matched models) and does not support causal or predictive inference.

Figures

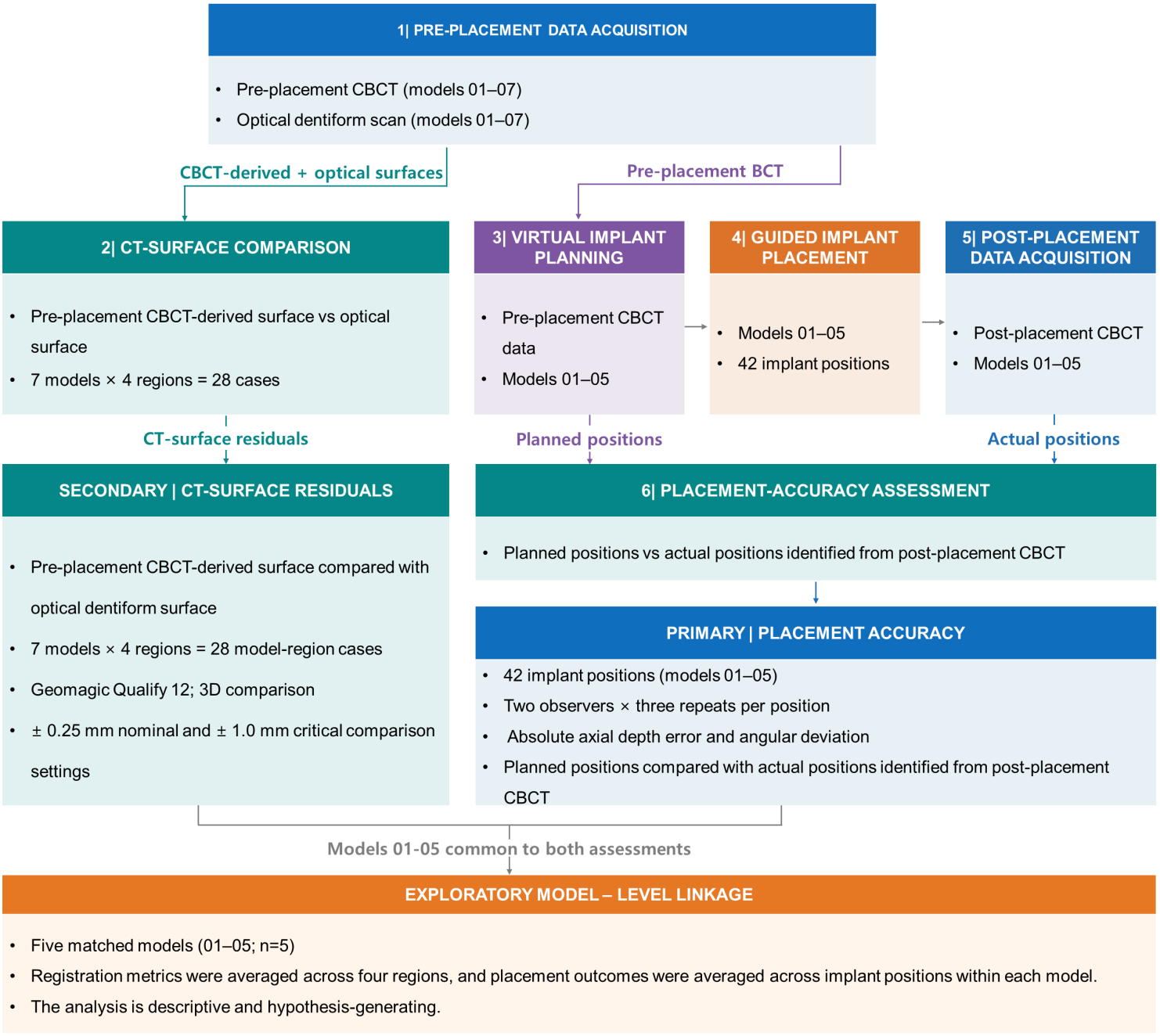


Figure 1

Overview of the bench-top study workflow. Pre-placement CBCT scans and optical surface scans were obtained for all seven dental models (models 01–07). The pre-placement CBCT datasets were used for CBCT–surface comparison across the seven models (four regions per model; 28 model–region cases) and for virtual implant planning in models 01–05. Surgical guides were designed and fabricated for models 01–05, in which guided implant placement was performed at 42 positions. After placement, models 01–05 were scanned again using CBCT; these post-placement datasets were used to identify and measure actual implant positions for the placement-accuracy analysis. CT–surface residuals were evaluated using the pre-placement CBCT and optical surface data, whereas placement accuracy was evaluated by comparing planned positions with actual positions identified from the post-placement CBCT data.

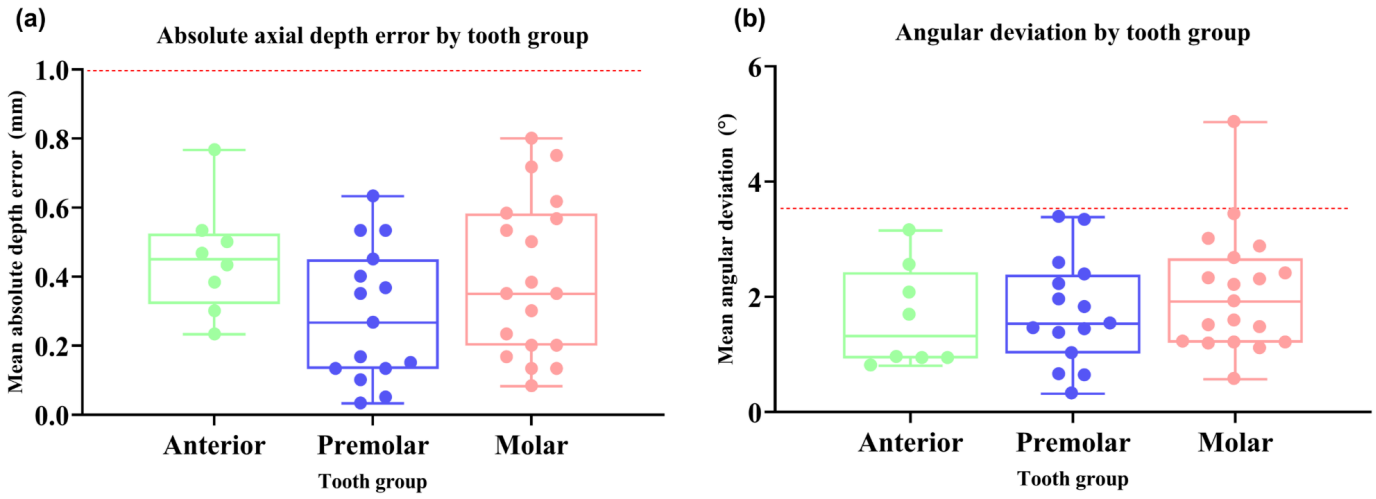


Figure 2

Position-level distributions of absolute axial depth error and angular deviation by tooth group. (a) Absolute axial depth error and (b) angular deviation. Each point represents one of 42 implant positions (anterior, n = 8; premolar, n = 15; molar, n = 19), with each value calculated as the mean of six readings (two observers × three repeats). Boxes show the interquartile range (25th–75th percentiles), center lines indicate medians, and whiskers extend from the minimum to the maximum. Red dashed lines indicate the study-specific placement reference criteria: ≤1.0 mm for absolute axial depth error and ≤3.5° for angular deviation; these are not universal clinical acceptance thresholds.

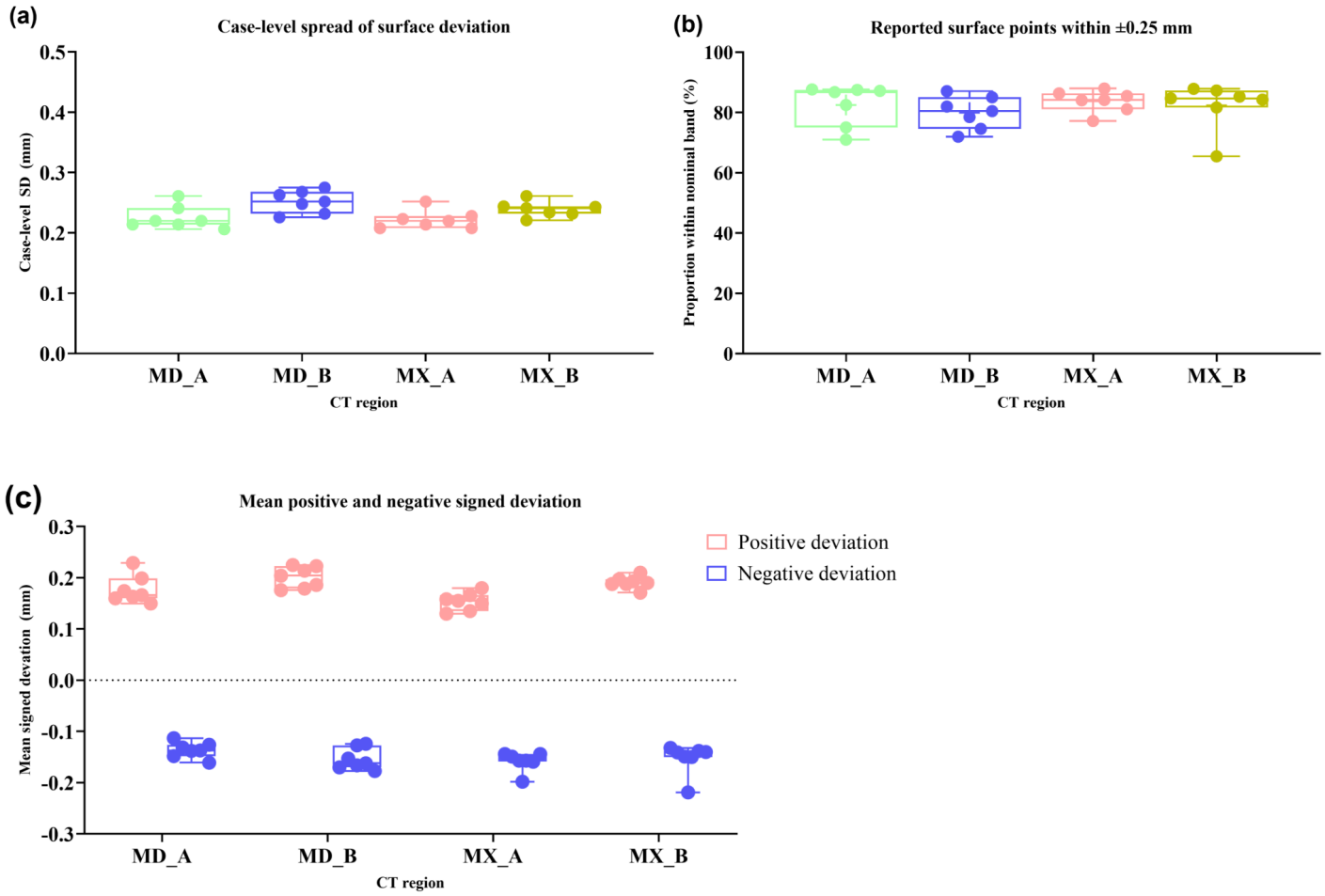


Figure 3

Case-level distributions of CT–surface comparison residuals by region. (a) Case-level standard deviation of surface deviation (mm); (b) percentage of reported surface points within ±0.25 mm; and (c) case-level mean positive and negative signed deviations (mm). Each point represents one model–region case summary, with seven models per region (n = 7 per region; 28 cases total); points do not represent individual mesh points. Boxes show the interquartile range (25th–75th percentiles), center lines indicate medians, and whiskers extend from the minimum to the maximum. In panel (c), coral and blue denote positive and negative deviations, respectively; the dotted horizontal line marks zero. The Geomagic output was limited to ±1.0 mm, so deviations beyond this range could not be assessed.

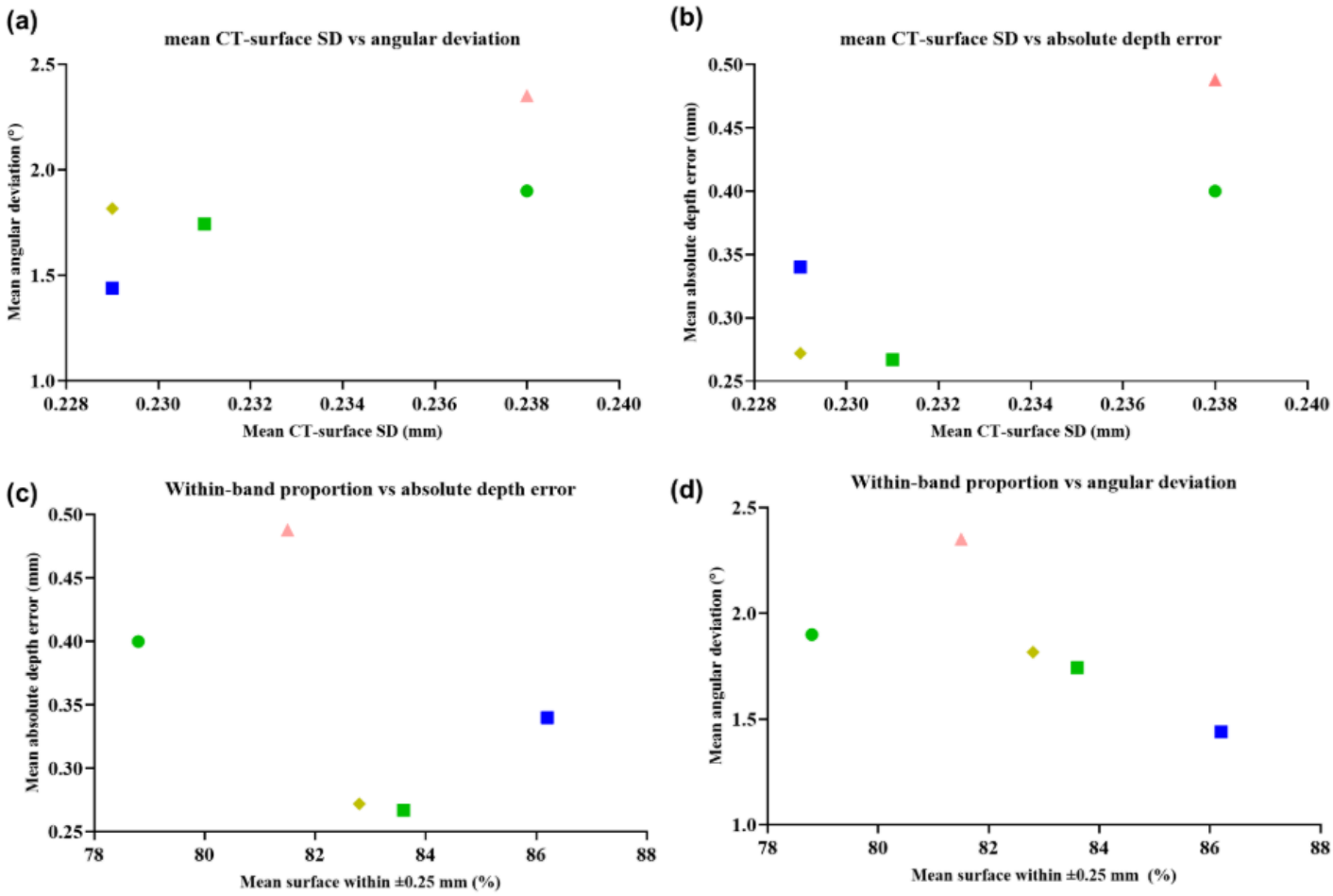


Figure 4

Exploratory model-level associations between CT–surface metrics and implant-placement outcomes in five matched dentiform models. Each point represents one model (n = 5); colors and symbols identify the same model consistently across panels. CT–surface metrics were averaged across the four regions, and placement outcomes were averaged across implant positions within each model. (a) Mean CT–surface standard deviation versus mean angular deviation (Spearman's ρ = +0.667; exact two-sided permutation P = 0.267); (b) mean CT–surface standard deviation versus mean absolute axial depth error (ρ = +0.667; P = 0.267); (c) mean percentage of reported surface points within ±0.25 mm versus mean absolute axial depth error (ρ = −0.600; P = 0.350); and (d) the same surface metric versus mean angular deviation (ρ = −0.900; P = 0.083). No regression lines are shown. All P values exceeded 0.05; these descriptive, hypothesis-generating results do not establish causation or predictive performance.

Supplementary Files

This is a list of supplementary files associated with this preprint. Click to download.

- SupplementaryTableCaptions.docx